Optimisation of Crushers in an Open-pit Coal Mine

ENGN4628 Optimisation and Control with Uncertainty and Constraints - Research Project Report

Christopher Tsirbas
u7143682

Lachlan Knoke
u7298351

Chithi Gunatilake
u7637857

Joshua Dunn
u5365782

***Abstract*—Open-pit coal mines typically feed crushers using truck–shovel haulage, where the cost of transport per tonne of ore is dominated by diesel, tire/drive-train wear, and labour costs on mine roads. Conventional dispatch and scheduling approaches optimise queues and shovel utilisation but treat truck speed and per-kilometre costs as fixed. In reality, there's a trade-off between speed and shorter cycle time versus the higher fuel usage and accelerated wear that faster speeds incur. This project formulates a minimum-cost network-flow model for a Queensland coal mine setting in which each road arc carries a speed and wear-aware cost per tonne term and a daily mass capacity. This project utilises a diagraph to represent open-pit coal mine geography, with the objective being to minimise the cost of meeting the crushers' demands by delivering them ore through trucks, which must traverse the diagraph subject to road costs and capacity constraints. Through this framing, this project analyses wear-aware throttling: deliberately slowing non-bottleneck arcs, thereby reducing fuel and maintenance costs without sacrificing output. This project found that optimising for cost not only prevented bottlenecks, but reduced the overall cost of meeting crusher demand by 4.92%. Overall it was concluded that this optimisation has use cases for both existing and new mines, but it's recommended that further work should be done for the model, such as discretising it in order to increase its utility and accuracy.**

I. Introduction

Truck–shovel haulage remains the dominant material-handling mode in open-pit coal mines, where unit cost is driven by diesel consumption, tire and drive-train wear, and labour on haul roads connecting pits to crushers. Classical research work optimises dispatching and short-term schedules to reduce shovel idle time and truck delays, but typically fixes speed policies and treats per-km costs as exogenous inputs [1], [2]. In practice, feasible haul speeds are a decision lever that trade cycle time against fuel burn and wear, with empirically nonlinear dependencies on speed, grade, and road condition (rolling resistance) [3]–[5]. Moreover, throughput is commonly limited at the crusher, so raising haul speed upstream of a saturated crusher raises unit cost without raising shipped tonnes so pushing upstream trucks faster after the bottleneck saturates raises overall cost ($/t) [2], [6].

Alongside classic dispatching, optimisation-based policies for truck–shovel systems compute target flows between loading and dumping locations from an optimisation layer and then execute them in operations. Smith, Linderoth and Luedtke show both a nonlinear average-flow model that embeds queueing and a time-discretised mixed-integer program, validated by discrete-event simulation, and they demonstrate that optimisation-driven flow targets outperform rule-based dispatch [7]. Building on that idea, this study keeps the planner-executor separation but changes the planning objective and the cost representation. The planner is a linear minimum-cost flow on a fixed digraph in which per-arc unit costs depend on speed and road quality, consistent with mine energy and wear evidence that links fuel and maintenance to speed, grade and rolling resistance [?]. Throughput is treated as bottleneck-limited at the crusher, so throttling on non-bottleneck arcs is allowed to reduce fuel and wear without reducing shipped tonnes, consistent with reported crusher-utilisation effects [?]. Network-flow formulations have also been used to couple production and haulage, showing that multicommodity or time-expanded graphs can capture capacities, blending and transport while remaining tractable with decomposition or specialised cuts [8], [9]. The output is route and throttling targets at planner scale that remain compatible with a separate dispatcher for truck-level timing. Network-flow formulations have also been used to couple production and haulage, showing that multicommodity or time-expanded graphs can capture capacities, blending, and transport while remaining tractable with decomposition or specialised cuts [8], [9]. At the energy and equipment level, comparative studies of truck haulage versus in-pit crushing and conveying quantify the large diesel share in mine-to-plant logistics and the sensitivity of unit energy to operating regime and rolling resistance, which supports modelling per-arc costs as energy and wear sensitive [10]. Finally, mine-to-crusher economic models calibrate how upstream decisions in blasting and haul propagate to crusher utilisation and costs, directly supporting the treatment of crushers as demand or bottleneck nodes in a haulage network [11].

Original Equipment Manufacturer guidance and field studies report that fuel per distance rises with speed in typical mine-haul ranges due to engine load, gearing, and modest aerodynamic effects, while maintenance and wear per distance for tires, brakes, and driveline tend to increase with a higher exponent due to thermal and mechanical stress. Both are aggravated by grade and poor underfoot conditions, that is high rolling resistance [3], [5]. Independent pavement and deflection studies show that stiffer surfaces reduce heavy-vehicle energy use, reinforcing the mechanism by which road quality multiplies fuel per tonne and effective capacity [12]. These findings motivate power-law speed sensitivities for fuel and wear and multiplicative road-quality factors in per-arc costs, as well as throttling policies that slow non-bottleneck arcs without reducing crusher feed.

A network-flow formulation in a Queensland coal context is adopted, using widely deployed truck classes to anchor payload and planning speed, and a documented local infrastructure reference (Curragh North single-flight overland conveyor, 20.3 km) to motivate realistic distances and steady plant feeds [13]. The optimisation is instantiated at the Curragh open-cut operation in the Bowen Basin. The model is a linear minimum-cost flow over a digraph with per-arc unit costs and capacities, and the speed policy affects both via calibrated elasticities.

II. System Model and Problem Definition

The optimisation is instantiated in a Queensland coal mine setting (Bowen Basin). Representative truck classes (The Komatsu 930E-5 and Cat 793F) provide payload and planning-speed bands, and Curragh North's 20.3 km single-flight overland conveyor provides an empirical reference for pit–to–plant distances and steady plant feeds [8]-[11], [13]. These sources anchor orders of magnitude for payload, haul speeds, and distances used to parameterise arc capacities and per-tonne costs. Overall, the figures derived from the research inputs are summarised in Table I.

Arc unit costs reflect speed-sensitive fuel and wear with multiplicative road-quality factors; arc capacities reflect planning speeds, grades, path length, and class-based constraints (straightness/condition). The following subsection specifies the mass-flow capacity function adopted for each road arc.

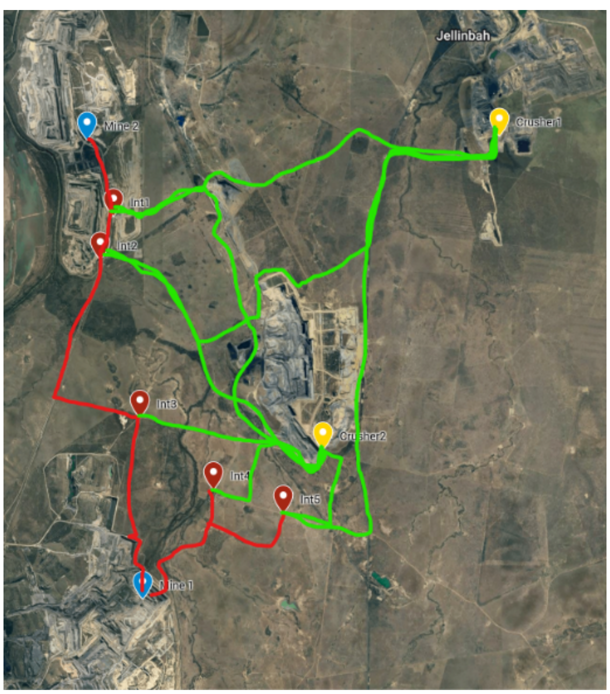

Fig. 1. Mine network digraph derived from Curragh Mine.

Overall, the figures derived from the project's research are shown in Table I.

A. Mass flow capacity function of a given road

$$Capacity(P_{i->j}) = \frac{1 - \frac{G}{25^\circ}}{q_{i,j}} * \frac{S_L * W_L}{d_{i,j}} | q_{i,j} \approx S_T \cdot R_C \quad (1)$$

In order to be able to describe the mass flow constraint equation of any given arc within the transport network, it was necessary to construct an equation that defined the maximum flow rate of material along that given arc. The main factors that are being considered to have an effect here are: the maximum permissible speed on the arc S_L, the effective gradient of the arc G, the practical weight limit that can be carried W_L, the length of the path $d_{i,j}$, and the classifications of the road in terms of condition and straightness (R_C and S_T respectively), which together correspond with the road quality factor $q_{i,j}$.

The equations that govern the majority of these factors are excessively complex for use case of this constraint equation, with many involving the solutions to partial differential equations, and so they have been replaced with first order approximations that give an adequate approximation on which to base the constraint factor.

The first factor to be considered is the speed limit. This is not necessarily just a legal speed limit but might also be a practical one, for example a large truck on a dusty road with a speed limit of 100 km/h. The legal limit may be 100, but the practical speed limitation that the truck would be under is far less, given that the trucks in question are not even capable of such speeds. Thus, the speed limit that would be used in the formula would be substantially lower. According to guidance from the Queensland government, the likely legal speed limit on this type of site would be 50-60 km/h [14]. Again, this is the legal upper maximum, not what may be practically permissible. This is a positively scaling factor, as completing a given route in a shorter time with a fixed load and route length would allow for more material to be carried in the same fixed time. This has units of km/h

The next factor is the effective gradient, which accounts for the changes in elevation that the truck would need to navigate along the route between the two nodes. This is not only the linear point to point gradient between the two nodes (the difference in elevation divided by the distance between them as the crow flies), as it also captures every vertical deviation along the route. The truck is power limited and unable to maintain its full speed on the way up any substantial hill, and on the way back down the hill, it'd likely have to brake, reducing the speed at which the truck completes the route. The true function would be an integral of the absolute value of all vertical deviations in the route between the two points. This has been approximated by the point to point gradient divided by the maximum gradient that the truck would be capable of navigating, given that the geography of the site is fairly simple. This is an inverse scaling factor, as there is no potential value that can speed up the truck. The range of values is defined as $0 < G < 25^{\circ}$, with units of degrees.

The next factor is weight limit. This is the result of three major factors, the number of trucks permitted through the route in a given time period, the trucks' capacity, and the geology and form of the road. Each truck has a maximum capacity which is restricted either by law or practical considerations. This defines an upper boundary on the load that can be carried on a single trip. However, this doesn't mean that this load can always be carried, as the road beneath the truck must also be able to support the ground pressure applied. Factors like how heavily packed the soil is, any recent rain or the presence of subterranean cavities will restrict how much pressure any travelling vehicle can apply. Erosion and the preservation of the road may also restrict the number of trucks that can pass through the arc in a given time. If allowing too many trucks to use the road too frequently results in excessive wear on the road, then it may be desirable to distribute the traffic flow across multiple paths. Weight limit is considered to be independent of the other factors, including road condition, and is a positive scaling factor, as a greater quantity carried on an otherwise fixed trip increases the material flow per unit time. This has units of tonnes.

The length of the arc is the linear distance the truck must go to navigate between two nodes. This is an inverse scaling factor, as increasing the length will take more time at the fixed speed, thus permitting fewer trips to be made per unit time.This has units of km.

The last two factors are the two road classifications in terms of road straightness and condition. These factors have been divided into three classes that'll apply a scaling factor onto material flow. They were modelled like this as they are less likely to be determined by physical limits such as truck speed around a corner before it topples or how fast the truck can hit a bump without damaging the suspension. Rather, they'll be the result of driver judgement or company policy based around previous experience and practicality. Road straightness is the measure of how many corners and bends the truck navigates on the given path. Cornering at great speeds is a substantial risk that could lead to injury and damage, and so drivers would be expected to slow down substantially, reducing average speed along the route. Similarly, a road littered with large rocks and potholes requires the driver to slow down and drive more carefully. The equation that quantifies the road roughness is $RI = 1 - 2STD(\frac{e}{c})$, with elevation mapping of the site (e) and the ground clearance of the vehicle (c) [15]. While this is a simple equation, it relies on terrain mapping and vehicle details, which aren't available for this project. It also doesn't account for driver behaviour or company policies, so a class system has been implemented instead. The scaling parameters associated with the classes are dimensionless inverse scaling factors.

Without the simplifications made, the mass flow capacity becomes very complex. The equation that governs the force on the vehicle is $F = R\dot{Z} + Z$. The dynamics of the vehicle are described by:
$\frac{1}{\omega_n^2}\ddot{P} + \frac{2\xi}{\omega_n}\dot{P} + P = \frac{2\xi}{\omega_n}\dot{Z} + Z$, $F = R\dot{Z} + Z$
Where F is the dynamic force on the vehicle frame, P is the vehicle mass motion, ω_n is the natural frequency of the system and ξ is the system damping ratio [15].

This is only part of the calculation that'd describe terrain roughness's effect on the vehicle. These are extensions to the project that could be enacted with full site access, the vehicles being used and the company policies enacted. Within this project, the effect of these two factors has been determined to be adequately similar to that of the road-quality multiplier used in the cost function. As such, this factor will be used in the constraint functions as well for consistency.

B. *Cost per tonne function of a given road*

The cost per tonne to move material along node $i \to j$ is represented as the sum of a fuel term and a maintenance/wear term accumulated over the arc distance. Both terms depend on the payload carried on that arc, the speed policy applied on that arc, and the road surface quality. Fuel and wear increase with higher gross load, higher speed, and higher total resistance from the road. Total resistance is the combination of grade resistance and rolling resistance; higher total resistance requires more power, which increases fuel use and tire and undercarriage costs. This motivates a multiplicative road-quality factor to reflect rolling resistance and curvature classes [5].

General form.

$$c_{i,j} = d_{i,j}\left(\gamma_{\text{fuel}}\left(\frac{S_L}{v_0}\right)^{\delta} + \gamma_{\text{maint}}\left(\frac{S_L}{v_0}\right)^{\gamma}\right) q_{i,j}. \qquad (2)$$

Here, $d_{i,j}$ is arc length [km], S_L is the effective speed policy on the arc [km/h] with v_0 a reference speed, $q_{i,j}$ is a road-quality multiplier that captures rolling resistance, curvature, and surface condition, and $\gamma_{\text{fuel}}, \gamma_{\text{maint}}$ are baseline coefficients per kilometre per transported tonne.

Fuel component.

$$c_{i,j}^{\text{fuel}} = d_{i,j}\, p_f\, \alpha_f \left(\frac{P_r}{P_0}\right)^{\eta} \left(\frac{S_L}{v_0}\right)^{\delta} q_{i,j}, \qquad (3)$$

where p_f is diesel price [\$/L], α_f is an effective $\mathrm{L\,km^{-1}\,t^{-1}}$ factor at (P_0, v_0), P_r is the average payload on the arc and P_0 a reference maximum payload. Empirical work in surface mining consistently identifies payload, truck speed, and haul-road condition as dominant predictors of haul-truck fuel consumption, with non-linear responses; this supports using elasticities on payload and speed calibrated from OEM curves or site telemetry [16]–[18].

Maintenance and wear component.

$$c_{i,j}^{\text{maint}} = d_{i,j}\,\beta_m\left(\frac{P_r}{P_0}\right)^{\zeta}\left(\frac{S_L}{v_0}\right)^{\gamma} q_{i,j}, \tag{4}$$

β_m is a baseline \$/km/t factor and ζ, γ are elasticities [19]–[21]. Industry practice uses TKPH, defined as mean tire load multiplied by average speed, as the standard site index for heat generation and allowable operating envelope. Increasing either variable raises operating TKPH and accelerates wear unless the other is reduced or road quality is improved, which motivates a multiplicative load-speed structure.

Combined form used in the model.

$$c_{i\to j} = d_{i,j}\Big[p_f\,\alpha_f\left(\frac{P_r}{P_0}\right)^{\eta}\left(\frac{S_L}{v_0}\right)^{\delta} + \beta_m\left(\frac{P_r}{P_0}\right)^{\zeta}\left(\frac{S_L}{v_0}\right)^{\gamma}\Big]\,q_{i,j}, \tag{5}$$

To parameterise the elasticities in (3) and (4), calibrated values are fixed within empirically supported bands from OEM guidance and field studies, matched to Bowen Basin Class II roads and 793F or 930E class fleets.

The fuel speed exponent is $\delta = 1.22$. Multiple field datasets and OEM frameworks show fuel per distance rises more than linearly with average haul speed in typical mine ranges. In a Cat 793 class telemetry study using 12 months of VIMS data, Soofastaei reports a convex increase in fuel index with average truck speed and with total resistance, illustrated around the results discussion and figures, which supports a super linear speed elasticity for fuel and quantifies penalties at higher speeds on rougher roads [18]. Caterpillar technical guidance formalises the mechanism that total resistance is the sum of grade and rolling resistances, and higher resistance at higher speed requires more power which increases fuel consumption. The same guidance links higher resistance to higher costs of fuel, tires and undercarriage [3], [5]. Given planning speeds are commonly 30 to 60 km/h on Class II mine roads in Bowen Basin operations and truck classes comparable to the study, a convexity band of $\delta \in [1.1, 1.3]$ is consistent with these sources; selecting $\delta = 1.22$ places the model in the middle of that empirical band while avoiding an overly aggressive penalty where aerodynamic effects remain modest [3].

Fuel payload exponent $\eta = 0.35$. When fuel is expressed per tonne kilometre, the elasticity with respect to payload is expected to be sub linear because gross mass increases tractive effort and fuel but the per tonne normalisation damps the response. Soofastaei and related surface mine studies emphasise payload, truck speed, and total resistance as dominant predictors of fuel. Together with the resistance framework, this motivates a payload elasticity below 1.0 in per tonne metrics [16]–[18]. In Queensland coal fleets, payload bands typically sit within the nominal ranges of the Komatsu 930E 5 and Cat 793F and operate on roads where rolling resistance varies with underfoot quality. In this regime a defensible prior is $\eta \in [0.2, 0.5]$; fixing $\eta = 0.35$ reflects noticeable tractive effort sensitivity to payload fraction while remaining compatible with the per tonne normalisation used in the model [16], [17].

The wear and maintenance speed exponent is $\gamma = 1.70$. Tire and running gear wear is strongly speed sensitive because thermal loading rises with carcass flexing frequency and power dissipated in the tire. Industry practice captures this with TKPH, defined as mean tire load multiplied by average speed; Bridgestone and other OTR databooks present this definition and operating derations which effectively limit allowable speed for a given load to maintain tire life [19]–[21]. Because TKPH is linear in speed at fixed load, and because empirical tire life response steepens as operating TKPH approaches the rating, a maintenance term with a speed elasticity steeper than the fuel term is appropriate. For Class II roads and Bowen Basin ambient conditions with 793F or 930E loads, a practical band is $\gamma \in [1.5, 2.0]$; $\gamma = 1.70$ reflects strong but not extreme speed sensitivity consistent with planned operations [19].

Wear and maintenance payload exponent $\zeta = 0.90$. The same TKPH framework implies a near linear dependence of operating severity on mean load at fixed speed; the data books make the load times speed product explicit and explain that exceeding the TKPH rating shortens tire life [19], [20]. Rolling resistance also increases with gross mass and underfoot deformation, reinforcing the load effect on heat generation and wear [5]. For Bowen Basin haul conditions with controlled payload variability in a 930E 5 or 793F fleet, a near linear elasticity ζ is defensible; fixing $\zeta = 0.90$ captures the strong load sensitivity while leaving modest headroom for non-linearity due to underfoot variability and duty cycle differences across arcs [5], [19].

With calibrated non-linear elasticities in place, the model evaluates the arc unit cost $c_{i\to j}$ using (5), where the fuel term scales super-linearly with speed and sub-linearly with payload in per-tonne units (empirically consistent with haul-truck telemetry and surface-mine studies), and the wear term carries a steeper speed sensitivity and near-linear load effect in line with TKPH practice [16]–[20]. The road-quality multiplier $q_{i,j}$ reflects grade and rolling resistance as standardised in OEM guidance on total resistance and its power/fuel implications [3]. For tractability at planning scale, speed policies are fixed scenario-by-scenario and $c_{i\to j}$ is precomputed for each arc and scenario, so the network problem remains a linear minimum-cost flow; sensitivity to speed can then be assessed by resolving the flow with alternative precomputed cost sets [3].

C. Problem Formulation

The planning horizon is one day. The haulage system is represented as a directed graph $G = (N, A)$ whose nodes N are pits (supplies), interchanges/stockpiles (transshipment), and crushers (demands), and whose arcs A are haul roads. The topology follows the site map in Fig. 2. Arc lengths $d_{i,j}$ are measured along mapped paths; node elevations and intermediate profile samples define an effective grade proxy G; curvature/straightness classes S_T come from plan geometry (bend count and turning radii); and underfoot condition R_C defines road quality. The road-quality multiplier $q_{i,j}$ aggregates curvature/underfoot effects in the total-resistance sense used by OEM guidance. Data sources and classing rules used to populate $d_{i,j}$, G, S_T, R_C, and $q_{i,j}$ are documented in Appendix A. Nominal pit–to–plant distances are anchored by the Curragh North 20.3 km single-flight conveyor benchmark for scale consistency with Bowen Basin operations; site lengths are read from survey/GIS and cross-checked against that benchmark.

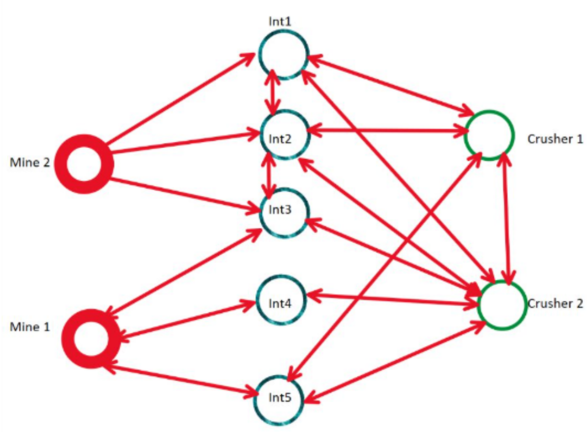

Fig. 2. Mine network digraph used in the model.

Per-arc unit costs $c_{i\to j}$ are precomputed from the fuel and wear model in Section II-B for the selected speed policy on each arc, and arc capacities $\mathrm{Capacity}(P_{i\to j})$ use the de-rated form in Eq. (1).

Table II lists the symbols and typical ranges used when populating the network parameters from survey/GIS and site/OEM sources.

Factor	Symbol	Typical Range
Weight Throughput Proxy	W_L	∼1250 t [22]
Fuel Price	p_{fuel}	\$1.2–\$2.0/L [23]
Actual Payload	P_r	220–290 t [22]
Maintenance Baseline	β_m	\$0.01–0.05/(km·t) [23]
Fuel Capacity Coefficent	α_{fuel}	0.02–0.06 L/(km·t) [24]

TABLE I
PARAMETERS, SYMBOLS, AND RANGES USED IN THE HAULAGE MODEL.

The distances between the nodes can easily be found on Google Earth. For our example mine we can calculate the gradients using the elevation data, also found on Google Earth **??**.

Factor	Symbol	Typical Range
Speed Limitation (km/h)	S_L	10–65 [24]
Road Straightness Class	S_T	Class II (typ.) [24]
Road Condition Class	R_C	Class II (typ.) [24]
Length of Route (km)	$d_{i,j}$	5–30 [24]
Gradient/Slope (degrees)	$G_{(i,j)}$	-1 to 1 degrees

TABLE II
PARAMETERS, SYMBOLS, AND RANGES FOR ROADS.

Let $V_{i\to j} \geq 0$ denote tonnes routed on arc $i \to j \in A$. The total cost of meeting crusher demands is

$$\min \sum_{(i,j)\in A} V_{i\to j}\, c_{i\to j}. \tag{6}$$

If the adjacency formulation is preferred, one may instead write $\min \sum_i \sum_j V_{i\to j} c_{i\to j} b_{i\to j}$.
Flows satisfy conservation at intermediate nodes, supply bounds at mines, demand at crushers, and arc capacity limits:

$$\sum_{j:(j,n)\in A} V_{j\to n} - \sum_{j:(n,j)\in A} V_{n\to j} = 0 \quad \forall \text{ intermediate } n \in N, \tag{7}$$

$$\sum_{j:(j,m)\in A} V_{j\to m} - \sum_{j:(m,j)\in A} V_{m\to j} \geq -V_{\text{initial}\,m} \quad \forall \text{ mine } m \in N, \tag{8}$$

$$\sum_{j:(j,c)\in A} V_{j\to c} - \sum_{j:(c,j)\in A} V_{c\to j} \geq V_c^{\text{demand}} \quad \forall \text{ crusher } c \in N, \tag{9}$$

$$0 \leq V_{i\to j} \leq \mathrm{Capacity}(P_{i\to j}) \quad \forall (i,j) \in A, \tag{10}$$

where $\mathrm{Capacity}(P_{i\to j})$ is given by Eq. (1). Feasibility requires that aggregate supply meet or exceed aggregate crusher demand and that each mine have at least one capacity-feasible path to a crusher; solver conflict reports identify tight arcs for potential upgrade or speed-policy relaxation.

Uncertainty in elasticities and prices is handled via three independent cases (lower, midpoint, upper), using the bounds in Table III. Each case reuses (6)–(10) and differs only in the precomputed $c_{i\to j}$ values (Section II-B) and in capacity inputs implied by the chosen speed policy and parameter set. Each case is solved as a linear program with a commercial LP/MIP.

Variable	Lower	Midpoint	Upper
γ	1.5	1.7	2.0
η	0.2	0.35	0.5
δ	1.1	1.22	1.3
α	0.02	0.04	0.06
Fuel price (\$/L)	1.2	1.6	2.0

TABLE III
SCENARIO BOUNDS USED IN THE PLANNER-HORIZON SOLVES.

To summarise the three scenario results, a three-point PERT estimate is used. Let O (optimistic) be the lower-bound outcome, M (most likely) the midpoint outcome, and P (pessimistic) the upper-bound outcome for the total cost. The PERT expected value is

$$\mathbb{E}[\mathrm{Cost}] = \frac{O + 4M + P}{6}, \tag{11}$$

and, when needed, the corresponding standard deviation proxy is $(P - O)/6$. The PERT roll-up for the reported experiments is computed from the scenario solve outputs and presented alongside the detailed route/capacity results. This project assumed that the lower and upper bound cases for the minimum cost were far less likely than the midpoint case, so PERT's use of a weight on the midpoint suited this assumption.

III. Proposed Solutions and Numerical Validations

A. *Solutions/system performance*

The optimum values of the minimum cost flow problem were evaluated through the program attached in Appendix B, which used the Gurobi package. The Gurobi package was selected as it made it easier to add flow constraints to the system. Using the midpoint and the lower and upper bounds of the variables in Table III, the system determined the optimal cost to meet the crushers' demands for each of these situations, and these results are shown in Table IV. In Table V, the mass flow through each of the roads are also shown for the midpoint case, along with the associated capacity and cost functions. In figure 3, the routes used by this optimisation are highlighted in green. The flowchart in figure 4 also shows the routes used. Using the PERT method, the simulated results produced a weighted mean of \$6659.8. Examining these figures, it's notable that the optimised solution doesn't use the quickest paths to crusher 2, which would've been m1->int4->crusher2. This highlights that this optimisation is focused on finding the minimum cost to meet demand rather than minimum distance.

Lower bound cost	Midpoint cost	Upper bound cost
\$2558	\$6448	\$11609

TABLE IV
Simulated costs to meet crusher demands while optimising for cost

Road	Mass through road (tonnes)	Road capacity (tonnes)
mine1 to int3	1275	4456
mine2 to int1	1024	16024
int1 to crusher1	1024	1024
int3 to crusher2	1275	9908
Crusher2 to crusher1	125	990

TABLE V
Mass flow through the roads used in the cost optimisation

In comparison, optimising the problem so that it minimises the time taken to meet crusher demands produces the results in Table VI, which produces a PERT estimate of \$7004.2. The routes used in this speed optimisation are shown in figure 5. The routes used here are notably different than figure 3, prioritising routes with the shortest distance. As a result, the crusher to crusher route is no longer used. In addition, int4 is now used to get to crusher 2 rather than int3. Overall, optimising for cost rather than speed reduces the cost to meet crusher demands by 4.92%. While this comes at the cost of time, this is actually an advantage, as it utilises throttled-bottle-necking.

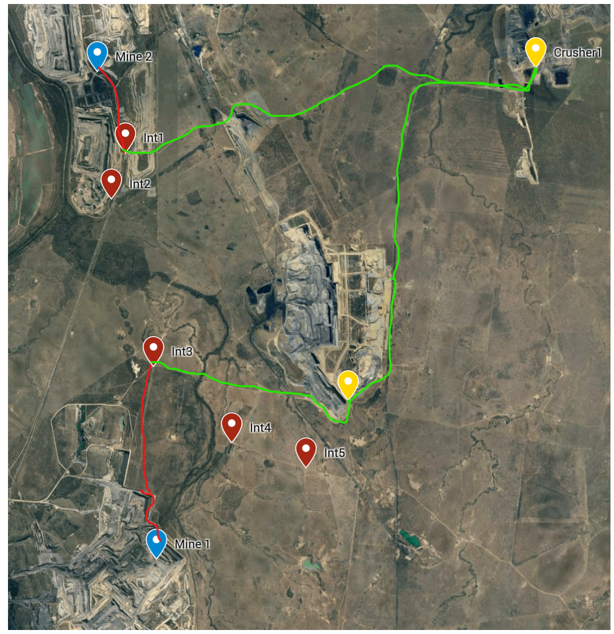

Fig. 3. Roads used in the cost optimised model.

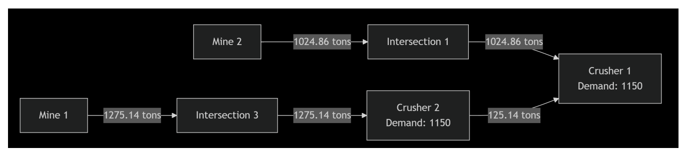

Fig. 4. Flowchart show the optimised mass flow.

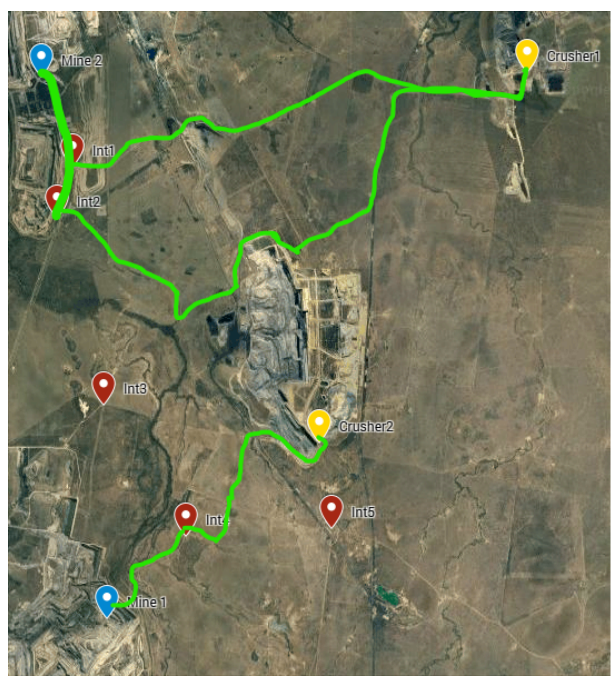

Fig. 5. Roads used in the speed optimised model.

Lower bound cost	Midpoint cost	Upper bound cost
$2720	$6785	$12135

TABLE VI
SIMULATED COSTS TO MEET CRUSHER DEMANDS WHEN OPTIMISING FOR SPEED

B. Validation

To validate the results of this simulation, the results were compared to estimations using real-world values. The following formula was used to compute these estimations of the cost per hour to meet crusher demands:

$$\begin{aligned} \text{Cost per hour (\$/hour)} &= \text{number of trucks}* \\ &(\text{fuel consumption(L/hour)} * \text{fuel price (\$/L)} \\ &* \text{road straightness} * \text{road curvature}) \\ &+(\text{Tires maintenance cost (\$/year)/364 days/12 working hours}) \end{aligned} \tag{12}$$

Table VII contains all the values that were used for the cost per hour estimates. Fuel usage per hour and tires maintenance cost per truck were obtained from Sunhunk, a mining equipment manufacturer [25]. The fuel price per litre uses the same range that the optimisation problem used in Table II. Finally, the range of numbers for the number of trucks was obtained by dividing the combined crusher demands of this problem (2300 tonnes) by the lower bound, midpoint and upper bound of the truck's reference payload (again from Table II). The road curvature and straightness values are the weighted average of the road curvatures and straightnesses associated with the roads used by the actual optimisation program (using the midpoint case). Table VIII shows the estimated costs per hour obtained via formula 12.

Variable	Lower bound cost	Midpoint cost	Upper bound cost
Number of haulage trucks	8	9	10
Fuel consumption (L/hour)	150	175	200
Fuel price ($/L)	1.2	1.6	2
Tire maintenance cost per truck ($/year)	300000	450000	600000

TABLE VII
VARIABLES AND THEIR RANGES USED FOR ESTIMATION

Lower bound cost	Midpoint cost	Upper bound cost
$3555	$6187	$9724

TABLE VIII
ESTIMATED COSTS PER HOUR VIA FORMULA 12

Using the PERT method, the estimated results produced a weighted mean of $6337.8. In comparison, the weighted mean from earlier was $6659.8. Overall, the estimated results largely validate the simulated results. The PERT estimates share the same order of magnitude, and only differ by $322, suggesting that the simulation is of good quality.

C. System limitations

The use of an optimisation such as this comes with several limitations and challenges. The first of these is a sufficiently accurate model. If the model used for a system has been oversimplified or there is some misunderstanding of the relationships involved in the system, then the model will likely not be representative of the real world system and the optimisation will not be accurate. For the model to be accurate, the model itself must be adequately representative (though no model is ever perfectly accurate, so compromise is always required), the model must have accurate values for the various contributing factors and the operating point of the system must be adequately close to any points of linearisation or approximation. As this project uses linearisation and approximation for both the capacity and cost functions, the project's system is not entirely accurate.

Furthermore, the system has not considered how it would operate under various conditions. For example, weather is not considered. Furthermore, the system has been structured so that mass flow can be modelled continuously. Over a large period of time, this assumption is reasonable, but at its core, the true system is discrete, as each chunk of ore is carried by a singular truck, and flow isn't continuous. Another limitation is the absence of time considerations within the system.

IV. FURTHER WORK

Further work for this project on other mining operations will require adapting the network representation to site geometry, recomputing arc lengths, grades, and curvature classes from survey or GIS, and recalibrating capacity and cost parameters using site telemetry and OEM guidance. Road quality multipliers should be re-estimated from rolling resistance and surface condition in line with total resistance practice, and TKPH envelopes should be checked against the tires in service to ensure feasible speed and load combinations [5], [26]–[28]. With these substitutions the linear minimum cost flow formulation remains unchanged and yields site specific throttling and routing guidance. Where truck level detail is required, add a short horizon time expanded MILP and validate it with a site calibrated discrete event simulator that uses the same network and demand inputs [29].

Further work that connects planner scale clarity to micro level realism should incorporate a discrete truck scheduling layer. The discrete alternative in the literature represents individual trucks over time using binary assignment, traversal lags, and explicit service times at shovels and crushers, and evaluates performance in a discrete event simulator [29]. A practical integration is to use the linear flow solution as a prior and lift it into a one to four hour time expanded network, seeding truck arc binary variables so that aggregated assignments match target flows on each arc and enforcing queuing at shovels and crushers [29]. This two layer workflow preserves planner scale transparency while gaining truck by truck movement fidelity in simulation.

Further work should also elevate speed from a parameter to a controlled variable in the discrete layer. Empirical studies and OEM handbooks show that fuel per distance grows more than linearly with average haul speed and that wear accelerates with the TKPH product of load and speed [5], [26]–[28], [30]. Per arc per interval speeds can be introduced with piecewise linear fuel and maintenance costs and with TKPH envelope constraints that couple allowable speed to load. Initial formulations can remain MILP for tractability and move to convex MINLP where accuracy gains justify solve time. Driving a discrete event simulator from the optimiser targets then makes crusher starvation and shovel queues explicit and allows fair comparisons across policy classes, including recent learning based dispatchers trained inside simulation [31].

Further work reapplying this to other mining sites should consider uncertainty in rolling resistance, road condition, truck availability, and fuel price using scenario bundles and a risk aware objective such as CVaR to stabilise speed choices under rougher underfoot conditions [32]. Where semi mobile IPCC is under consideration, the time expanded model can be augmented with binary on and off choices for IPCC segments and relocation costs so that truck throttling, crusher feed targets, and IPCC placement are optimised in one view [10]. This optimisation and the associated formulation has a reasonably broad range of application. In order to apply this to another existing mine, some changes would need to be made, including a new network map based around the specific layout of the new mine, calculating the new arc cost values and calculating the new capacity constraint functions for each arc. This would allow for the rest of the model to be applied broadly intact. If the model was to be used to optimise the layout of a new mine that has not been constructed, then some additional work would be required in the laying out of the network map. Depending on the geography and geology of the site, it may be possible to simply lay a pattern of rectangular or hexagonal polygons over the whole site, with nodes at each vertex, then eliminate nodes based around obstructions, before proceeding as before. The calculation of the cost and constraint for each arc may become complicated using this method, but it'd likely be possible to obtain these procedurally based on topographical maps of the area. This form of optimisation could allow the planners of the new mine to produce the mine with the minimum viable infrastructure, thereby reducing the cost of construction and allowing resources to be focused on the areas where they'll produce the most benefit.

V. Conclusion

The goal of this project has been to optimise the route taken by the trucks within a coal mine to minimise the transport cost of the material to be crushed while also mitigating bottle-necking. This has been effectively achieved through the application of a network flow optimisation with static arc costs and flow capacity constraints. The method applied was able to produce meaningful figures for the estimated operation cost for material transport, along with PERT analysis for that cost. The limitations of this optimisation system are based on the accuracy of the model applied, the data quality and the distance between the point of linearisation and the point of operation. The optimisation model developed here has several use cases, ranging from the optimisation of existing mines or the layout of new mines to the optimisation of material transport within factories. There is potential for further work that could be done, such as reworking the model as a discrete or mixed integer optimisation which would further expand its utility and enhance its accuracy.

References

[1] S. L. Smith, J. Linderoth, and J. Luedtke, "Optimization-based dispatching policies for open-pit mining," *Optimization and Engineering*, vol. 22, no. 4, pp. 1347–1387, 2021. [Online]. Available: https://link.springer.com/article/10.1007/s11081-021-09628-w

[2] Vericom, "Rolling resistance plays a critical role in getting your job done," 2016, white paper. [Online]. Available: https://www.vericomllc.com/images/VM-White-Papers/Rolling-Resistance-Plays-a-Critical-Role-in-Getting-Your-Job-Done.pdf

[3] Caterpillar Inc., "Cat performance handbook, edition 50," 2022, haul-road, grade and rolling-resistance guidance. [Online]. Available: https://www.cat.com/en_US/by-industry/surface-mining/performance-handbook.html

[4] Continental Industry, "Conveyor belt solutions for every mining task," 2019. [Online]. Available: https://www.continental-industry.com/getmedia/3cd2764e-6591-4274-b2f0-1dbe3d8a31b5/CBG0110-EN-Mining-Brochure.pdf

[5] Caterpillar Inc., "Rolling resistance factors," 2020, oEM explainer on grade and rolling resistance effects on power, fuel and wear. [Online]. Available: https://www.cat.com/en_US/articles/ci-articles/rolling-resistance-factors.html

[6] O. Online, "A review of dispatch models for truck–shovel systems in open-pit mining," 2020, preprint repository entry (topical review landing page). [Online]. Available: https://www.optimization-online.org/

[7] S. L. Smith, J. Linderoth, and J. Luedtke, "Optimization-based dispatching policies for open-pit mining," *Optimization and Engineering*, vol. 22, no. 4, pp. 1347–1387, 2021, foundational dispatch paper linking an optimization layer to real-time execution. [Online]. Available: https://link.springer.com/article/10.1007/s11081-021-09628-w

[8] A. Lamghari and R. Dimitrakopoulos, "Network flow-based algorithms for scheduling production in multi-processor open-pit mines accounting for metal uncertainty," *European Journal of Operational Research*, vol. 253, no. 3, pp. 843–855, 2016. [Online]. Available: https://www.sciencedirect.com/science/article/pii/S0377221716302013

[9] R. Goodfellow and R. Dimitrakopoulos, "Global optimization of open-pit mining scheduling with geological uncertainty," *European Journal of Operational Research*, vol. 222, no. 3, pp. 623–632, 2013. [Online]. Available: https://www.sciencedirect.com/science/article/pii/S0377221712003925

[10] D. Ritter, K.-D. Rinne, C. Willeke, D. Bornoff, and J. Hofmann, "A comparison of truck based material transport to in-pit crushing and conveying (ipcc) under deepening and widening conditions in a south african gold mine," in *Mine Planning and Equipment Selection*, S. U. Dikmen and Y. Kose, Eds. Cham: Springer, 2021, pp. 265–278, energy/cost comparison of truck haulage vs. IPCC. [Online]. Available: https://www.tib.eu/en/search-discover/document/243589323/A-comparison-of-truck-based-material-transport-to

[11] J.-H. Park, Y.-J. Choi, Y.-S. Choi, and K.-J. Kim, "Deep neural network for ore production and crusher utilization in truck haulage operations," *Applied Sciences*, vol. 9, no. 19, p. 4180, 2019, mine-to-crusher

operational coupling via data-driven modeling. [Online]. Available: https://www.mdpi.com/2076-3417/9/19/4180
[12] J. E. Sias, M. Akbarian, and F.-J. Ulm, "Pavement-vehicle interaction (pvi)—fuel consumption and tire wear on pavements," MIT Concrete Sustainability Hub, Tech. Rep., 2012. [Online]. Available: https://cshub.mit.edu/sites/default/files/2022-09/MIT_CSHub_PVI.pdf
[13] H. Abbaspour and C. Drebenstedt, "In-pit crushing and conveying systems in open pit mining," in *Advanced Surface Mining*, R. Singh and C. Drebenstedt, Eds. Cham: Springer, 2019, pp. 197–226, comprehensive IPCC overview; use as comparative baseline. [Online]. Available: https://link.springer.com/chapter/10.1007/978-3-319-76130-0_9
[14] Queensland Department of Transport and Main Roads, "Guide to speed management," 2025, state guidance on setting speed limits. [Online]. Available: https://www.publications.qld.gov.au/ckan-publications-attachments-prod/resources/2a65a8e5-453e-4aa7-b2f2-3e2e16a2bf7e/guide-to-speed-management.pdf
[15] A. El-Kabbany and A. Ramírez-Serrano, "Terrain traversability index for off-road vehicles," *International Journal of Intelligent Automation and Soft Computing*, vol. 16, no. 4, pp. 403–416, 2010. [Online]. Available: https://www.worldscientific.com/doi/abs/10.1142/S0218830110005355
[16] M. Sánchez, D. Sáez, E. Contreras, and E. Delgado, "A comparison of the fuel consumption and truck models in different open-pit mining projects," *Applied Sciences*, vol. 13, no. 9, p. 5769, 2023. [Online]. Available: https://www.mdpi.com/2076-3417/13/9/5769
[17] O. Golbasi and E. Kına, "Haul truck fuel consumption modeling under random operating conditions: A case study," *Transportation Research Part D: Transport and Environment*, vol. 102, p. 103135, 2021. [Online]. Available: https://www.sciencedirect.com/science/article/pii/S1361920921004302
[18] A. Soofastaei, S. M. Aminossadati, M. S. Kizil, and P. Knights, "The effect of average truck speed on fuel consumption in surface mines," 2016, cRCMining/UQ Mining Industry paper. [Online]. Available: https://soofastaei-publications.com/wp-content/uploads/2022/06/The-effect-of-average-truck-speed-on-fuel-consumption-in-surface-mines.pdf
[19] Bridgestone Corporation, "Off-the-road (otr) tire databook," 2018, tKPH guidance and site/tire TKPH calculations. [Online]. Available: https://commercial.bridgestone.com/content/dam/bcs-sites/bridgestone-ex/products/Databooks/Archive/Bridgestone-OTR-Databook-2018-09-06-2018.pdf
[20] Eurotire, "Bias & radial technical databook," 2013, tKPH/TMPH definition and site calculation procedure. [Online]. Available: https://otrtires.com/wp-content/uploads/23-DATABOOK-EN-031513.pdf
[21] BKT Tires, "Otr technical databook (international standard), 2024 edition," 2024. [Online]. Available: https://www.bohnenkamp.lv/catalogs/BKT_OTR_Technical_Databook_2024_IS_en.pdf
[22] *Caterpillar 794 AC Mining Truck Specifications*, Caterpillar Inc., 2024. [Online]. Available: https://www.cat.com/en_US/by-industry/mining/minexpo2024/products/productivity-class-trucks.html
[23] K. Ltd., "How to reduce haul truck fuel consumption," 2023. [Online]. Available: https://www.komatsu.com/en-us/case-studies/reduce-haul-truck-fuel-consumption
[24] S. C. Bhunia, "Unit operations in mining: Surface mining," *Academia*, 2019. [Online]. Available: https://www.academia.edu/40889634/UNIT_OPERATIONS_IN_MINING_SURFACE_MINING
[25] Sunhunk, "Why are mining haul trucks so expensive," 2025. [Online]. Available: https://www.sunhunk.com/about/groupnews-detail-588.htm
[26] Caterpillar Inc., "Cat performance handbook, edition 50," 2022, dealer-hosted PDF mirror of Edition 50. [Online]. Available: https://wheelercat.com/wp-content/uploads/2025/03/Cat-Performance-Handbook-Edition-50-June-2022.pdf
[27] Bridgestone Corporation, *Off-The-Road (OTR) Tire Databook*, 2018. [Online]. Available: https://commercial.bridgestone.com/content/dam/bcs-sites/bridgestone-ex/products/Databooks/Archive/Bridgestone-OTR-Databook-2018-09-06-2018.pdf
[28] BKT Tires, *OTR Technical Databook (International Standard), 2024 Edition*, 2024. [Online]. Available: https://www.bohnenkamp.lv/catalogs/BKT_OTR_Technical_Databook_2024_IS_en.pdf
[29] S. C. Smith, J. Linderoth, and J. Luedtke, "Optimization-based dispatching policies for open-pit mining," *Optimization and Engineering*, vol. 22, no. 4, pp. 1347–1387, 2021. [Online]. Available: https://link.springer.com/article/10.1007/s11081-021-09628-w
[30] A. Soofastaei, S. M. Aminossadati, M. S. Kizil, and P. Knights, "The effect of average truck speed on fuel consumption in surface mines," 2016. [Online]. Available: https://soofastaei-publications.com/wp-content/uploads/2022/06/The-effect-of-average-truck-speed-on-fuel-consumption-in-surface-mines.pdf
[31] V. Mukundan and A. Narayan, "Deep reinforcement learning based truck dispatcher for open-pit mines," in *AAAI 2025 Workshop on Optimization and Machine Learning for Applied Problems*, 2025, evaluated in a discrete-event simulator. [Online]. Available: https://womapf.github.io/aaai-25/pdf/Submission_23.pdf
[32] H. Amankwah, T. Larsson, and B. Textorius, "Open-pit mining with uncertainty: A conditional value-at-risk approach," in *Optimization Theory, Decision Making, and Operations Research Applications*, ser. Springer Proceedings in Mathematics & Statistics, A. Migdalas, A. Sifaleras, C. K. Georgiadis, J. Papathanasiou, and E. Stiakakis, Eds. Springer, 2013, vol. 31, pp. 117–139. [Online]. Available: https://link.springer.com/chapter/10.1007/978-1-4614-5134-1_8

APPENDIX A
DATA SOURCES AND CLASSING RULES USED TO POPULATE $d_{i,j}$, G, S_T, AND R_C

G and $d_{i,j}$ were derived from cartographical data. In Appendix D, the gradients and distances of all the roads are shown.

APPENDIX B
COST OPTIMISATION CODE

The Python Package can be found at this repository: https://github.com/lachlanknoke/engn4628-optimisation-assignment.

APPENDIX C
ELEVATION TABLE

Node	Elevation
Mine1	146m
Mine2	125m
Int1	138m
Int2	135m
Int3	138m
Int4	140m
Int5	162m
Crusher1	137m
Crusher2	155m

TABLE IX

Appendix D
Distance and Gradient Table

Road	Distance (km)	ΔElevation (m)	Gradient (%)	Gradient (°)
M2 $\rightarrow$ Int1	2.31	+13	0.56%	0.32°
Int1 $\rightarrow$ C1	15.12	-1	-0.07%	-0.04°
Int1 $\rightarrow$ C2	16.93	+17	0.10%	0.06°
Int1 $\rightarrow$ Int2	1.83	-3	-0.16%	-0.09°
Int2 $\rightarrow$ C1	19.89	+2	0.10%	0.06°
Int2 $\rightarrow$ C2	11.86	+20	0.17%	0.10°
Int2 $\rightarrow$ Int3	8.07	+3	0.04%	0.02°
Int3 $\rightarrow$ C2	7.53	+17	0.23%	0.13°
Int3 $\rightarrow$ M1	7.65	+8	0.10%	0.06°
Int4 $\rightarrow$ C2	8.59	+15	0.17%	0.10°
Int4 $\rightarrow$ M1	6.72	+6	0.09%	0.05°
Int5 $\rightarrow$ C1	21.10	-25	-0.12%	-0.07°
Int5 $\rightarrow$ C2	3.37	-7	-0.21%	-0.12°
Int5 $\rightarrow$ M1	9.71	+16	0.16%	0.09°
C1 $\rightarrow$ C2	15.65	+18	0.12%	0.07°
M1 $\rightarrow$ Int3	7.65	-8	-0.10%	-0.06°
M1 $\rightarrow$ Int4	4.02	-6	-0.15%	-0.09°
M1 $\rightarrow$ Int5	9.71	+16	0.16%	0.09°

TABLE X
Calculated Gradients for all Road Segments

Declaration: Chatgpt was used in this report.